

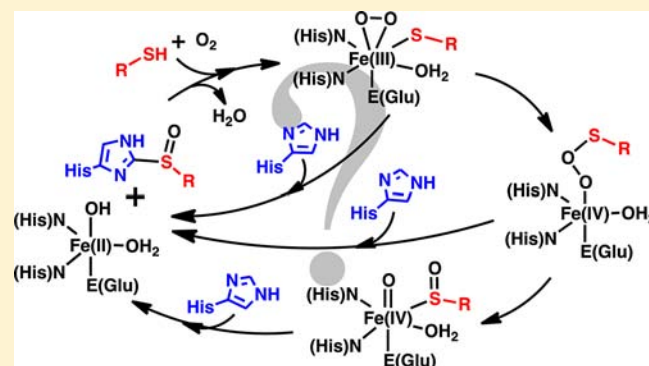
## Model Iron–Oxo Species and the Oxidation of Imidazole: Insights into the Mechanism of OvoA and EgtB?

Eric A. C. Bushnell, Grant B. Fortowsky, and James W. Gauld\*

Department of Chemistry and Biochemistry, University of Windsor, Windsor, Ontario N9B 3P4, Canada

## Supporting Information

**ABSTRACT:** A density functional theory cluster and first-principles quantum and statistical mechanics approach have been used to investigate the ability of iron–oxygen intermediates to oxidize a histidine cosubstrate, which may then allow for the possible formation of 2- and 5-histidylcysteine sulfoxide, respectively. Namely, the ability of ferric superoxo ( $\text{Fe}^{\text{III}}\text{O}_2^{\bullet-}$ ),  $\text{Fe}^{\text{IV}}=\text{O}$ , and ferrous peroxysulfur ( $\text{Fe}^{\text{III}}\text{OOS}$ ) complexes to oxidize the imidazole of histidine via an electron transfer (ET) or a proton-coupled electron transfer (PCET) was considered. While the high-valent mononuclear  $\text{Fe}^{\text{IV}}=\text{O}$  species is generally considered the ultimate biooxidant, the free energies for its reduction (via ET or PCET) suggest that it is unable to directly oxidize histidine's imidazole. Instead, only the ferrous peroxysulfur complexes are sufficiently powerful enough oxidants to generate a histidyl-derived radical via a PCET process. Furthermore, while this process preferably forms a  $\text{HisN}_\delta(-\text{H})^\bullet$  radical, several such oxidants are also suggested to be capable of generating the higher-energy  $\text{HisC}_\delta(-\text{H})^\bullet$  and  $\text{HisC}_\epsilon(-\text{H})^\bullet$  radicals. Importantly, the present results suggest that formation of the sulfoxide-containing products (seen in both OvoA and EgtB) is a consequence of the reduction of a powerful  $\text{Fe}^{\text{III}}\text{OOS}$  oxidant via a PCET.



## INTRODUCTION

Activation of dioxygen is well-established as a key physiological approach to, for instance, activation of metabolites and incorporation of oxygen into biomolecules.<sup>1,2</sup> Within cells, this process is typically catalyzed by enzymes that depend on metal cofactors, e.g., copper and iron.<sup>3,4</sup> Commonly formed intermediates in dioxygen activation by iron-containing metalloenzymes include the high-valent oxoferryl  $\text{Fe}^{\text{IV}}=\text{O}$ -containing species' compounds I and II (Cpd I and II, respectively) in heme enzymes<sup>5</sup> and Cpd II analogues in nonheme enzymes.<sup>4–12</sup> These moieties are generally considered to be the “ultimate biochemical oxidants”<sup>5,6,12–14</sup> with their reactivity tuned by such factors as the redox potential and spin state of the metal–oxo moiety.<sup>15</sup> Indeed, as a result, they are able to transform relatively stable bonds, e.g., C–H, via oxygen insertion.<sup>15</sup> Because of their preference for a high-spin ground state (GS), which thus allows for exchange enhanced reactivity, it has been stated that nonheme  $\text{Fe}^{\text{IV}}=\text{O}$  species exhibit greater reactivity than their heme analogues, which prefer a low-spin GS.<sup>16</sup>

For instance, 5-histidylcysteine sulfoxide synthase (OvoA) and 2-histidyl- $\gamma$ -glutamyl cysteine sulfoxide synthase (EgtB) are two nonheme iron-containing enzymes that activate dioxygen as part of their catalytic mechanism.<sup>17</sup> More specifically, they use dioxygen, histidine, and a cysteine derivative as cosubstrates to synthesize their respective sulfoxides.<sup>17,18</sup> The active sites of both enzymes utilize a conserved iron binding motif, which is

also common among dioxygen-activating enzymes,<sup>19</sup> involving two histidylimidazoles and a carboxylate side chain in a facial ligation.<sup>17,20</sup> Such an arrangement leaves several possible sites for iron–substrate binding. Because of these similarities in the reactants, product, and active site, it has been proposed that OvoA and EgtB share similar chemistry.<sup>20</sup> However, their exact catalytic mechanisms are unknown.

OvoA is found in marine organisms<sup>21,22</sup> such as sea urchins, scallops, starfish, and the annelid *Platynereis dumerilii*<sup>20,23</sup> as well as human pathogenic parasites of the *Trypanosoma* genus.<sup>20,24</sup> In the case of EgtB, it is found in nonyeast fungi, mycobacteria, and cyanobacteria.<sup>25</sup> Importantly, the products of OvoA and EgtB (hereafter referred to as 5- and 2-HisCysSO, respectively) are later converted to OSH and ESH (both of which are mercaptohistidine derivatives) to provide essential protection against oxidative damage. In particular, ESH has been shown to scavenge reactive oxygen species and radicals such as singlet oxygens, hydroxyl radicals, hypochlorous acid, and peroxyl radicals.<sup>26–31</sup> Importantly, ESH's medical potential is very promising where aerosols have been developed to treat chronic inflammatory diseases such as asthma.<sup>32–34</sup> Furthermore, it has been stated that ESH is an important chemoprotector present in humans.<sup>35</sup> It is noted that OSH, while an important antioxidant, has been suggested to have additional

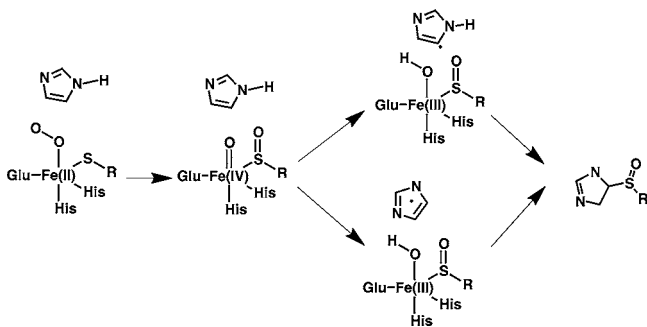
Received: September 28, 2012

Published: December 5, 2012

physiological roles.<sup>20</sup> For example, it has been proposed to act as a male pheromone in *P. dumerilii*.<sup>20,23</sup> Consequently, because of its wide presence in many organisms, the antioxidant and scavenging abilities of OSH have been studied extensively.<sup>17,21,24,36–43</sup>

The proposed mechanism of OvoA (Scheme 1), i.e., synthesis of 5-HisCysSO, begins with dioxygen and cysteine

**Scheme 1. Proposed Mechanism for the Formation of a Histidyl Sulfoxide via a Radical Mechanism, with Coupling between the Sulfoxide and Histidyl Occurring at the Latter's C $\delta$  Position (i.e., Synthesis of 5-HisCysSO)<sup>17</sup>**



binding to the ferrous ( $\text{Fe}^{\text{II}}$ ) center to form an  $\text{Fe}^{\text{III}}\text{O}_2^{\bullet-}$ -containing complex.<sup>17</sup> The latter species then attacks the iron-bound cysteine, homolytically cleaving its O–O bond with the formation of a sulfoxide $\cdots\text{Fe}^{\text{IV}}=\text{O}$  complex. Three possible pathways have been proposed for the next step.<sup>17</sup> In one, the histidine nucleophilically attacks at the sulfoxide sulfur center with concomitant deprotonation of  $\text{N}_\delta$  to directly give the product (not shown).<sup>17</sup> In the alternate two pathways, however, the histidine is oxidized via a proton-coupled electron transfer (PCET) onto the  $\text{Fe}^{\text{IV}}=\text{O}$  moiety. Specifically, a  $\text{H}^\bullet$  radical is abstracted from either its  $\text{C}_\delta\text{--H}$  or  $\text{N}_\delta\text{--H}$  groups to form an  $\text{sp}^2$  C-centered or a  $\pi$ -delocalized radical, respectively (Scheme 1).<sup>17</sup> The resulting histidyl radical is suggested to then attack the iron-bound sulfoxide to give the final product. However, a number of key questions remain including the nature of the oxidizing nonheme iron species and its coordination environment, the most likely histidyl radical resulting from oxidation, and the apparent need for the formation of a sulfoxide-containing intermediate when it is not present in the final product (i.e., OSH or ESH).

Thus, using a density functional theory (DFT) cluster approach in combination with a first-principles quantum and statistical mechanics<sup>44</sup> approach, we have computationally investigated the half-reactions for the oxidation of imidazole (Im) and the reduction of several possible iron–oxygen complexes via electron transfer (ET) or PCET. It is noted that because there are currently no available X-ray crystal structures for OvoA or EgtB the use of small model iron complexes herein does not provide a conclusive answer to the mechanisms of OvoA or EgtB. In particular, it does not explicitly account for the environmental effects provided by the secondary shell of active site residues within the respective enzymes. However, such a model approach can provide fundamental insight into the changes in the oxidative power of the iron center as the coordination around the center is changed. Specifically, we investigated 21 possible iron cluster models (i.e., the oxidized and reduced forms). For each of

these, we considered several possible multiplicities to give a total of 196 different iron complexes.

## COMPUTATIONAL METHODS

As noted above, there are currently no available X-ray crystal structures for OvoA or EgtB; thus, we have chosen to investigate seven possible models differing in their iron coordination arrangements (Figure 1). In

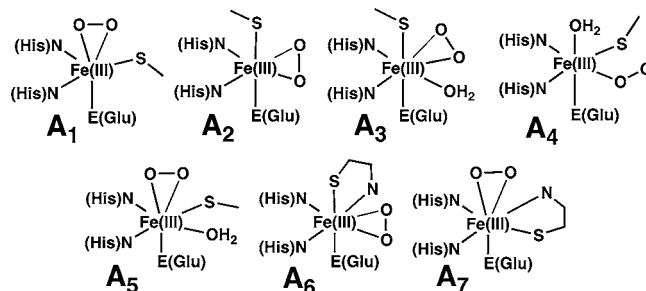


**Figure 1.** Initial five- and six-coordinate  $\text{Fe}^{\text{III}}\text{O}_2^{\bullet-}$  complexes considered herein.

all complexes, the ligating glutamate was modeled as formic acid. The ligating histidines were modeled as Im's. In all models, these residues ligate the iron center in a facial arrangement. For  $\text{A}_1\text{--A}_3$  complexes, methylthiol was used to model the ligating cysteine. In the case of  $\text{A}_1$  and  $\text{A}_2$ , we have modeled a five-coordinate iron center. For these complexes, the thiol was either cis or trans to the formate ligand, respectively. For  $\text{A}_3\text{--A}_5$ , we have modeled a six-coordinate iron center where water was added to fill the sixth coordination site of the metal. For these complexes, we have generated initial complexes such that the  $\text{MeS}^-$ ,  $\text{H}_2\text{O}$ , or  $\text{O}_2$  were trans to the carboxylate ligand, respectively. In the case of  $\text{A}_6$  and  $\text{A}_7$ , 2-aminomethylthiol was used to model a bidentately ligating cysteine. The difference between these two was whether the thiol was trans or cis to the carboxylate ligand. It is noted that for EgtB, which uses  $\gamma$ -glutamylcysteine as a substrate, the coordination modes for  $\text{A}_6$  and  $\text{A}_7$  are unlikely.

For the calculation of the half-reaction free energies, a DFT cluster model was used in combination with a first-principles quantum and statistical mechanics approach.<sup>44</sup> For the reactions considered herein, the protons and electrons were treated as independent ions. Thus, their chemical potentials have been taken to be that of a solvated free electron with respect to a standard hydrogen electrode (SHE) reference state ( $-418.5 \text{ kJ mol}^{-1}$ ) and a proton in a dilute aqueous environment ( $-1124.2 \text{ kJ mol}^{-1}$ ), as previously obtained by means of a first-principles quantum and statistical mechanics approach.<sup>44</sup>

For the remaining species (i.e., Im and iron complexes), the Gaussian 09<sup>45</sup> suite of software was used. In the present investigation, we have chosen to use the 6-31G(d) basis set on all atoms including iron (i.e., an effective core potential basis set for iron was not used). As a test, we ran the septet **A** complexes in Figure 1 (the reason being that they were the favored starting complexes; see below) and found the root-mean-square deviation in the  $\text{Fe--O}_2$  and  $\text{Fe--S}$  bond lengths to be  $0.04 \text{ \AA}$  with the SDD effective core potential basis set for iron, while the 6-31G(d) basis set was used for all other atoms. This combination of basis sets has been shown to be reliable in both mono- and binuclear iron-containing enzymes.<sup>46,47</sup> Furthermore, the bonding of the dioxygen (i.e., whether end-on or side-on was preferred) was identical between the basis sets used. Thus, it is believed that the differences in using the 6-31G(d) basis set solely would not significantly affect the key results obtained herein. Thus, the optimized structures and Gibbs corrections ( $\Delta G_{\text{corr}}$ ) were obtained at the B3LYP/6-31G(d) level of theory.<sup>48–53</sup> Relative energies were obtained via single-point calculations at the IEF-PCM-B3LYP/6-311G(2df,p)//B3LYP/6-31G(d) +  $\Delta G_{\text{corr}}$  level of theory.<sup>54–57</sup> In addition, single-point energies were also calculated using the IEF-PCM-M06/6-311G(2df,p)//B3LYP/6-31G(d) +  $\Delta G_{\text{corr}}$  method.<sup>58,59</sup> However, the results obtained were qualitatively similar to those obtained with the

B3LYP functional and thus, while provided in the following tables (in parentheses), are not discussed. Diffuse functions were not used because, as discussed by Martin et al.,<sup>60</sup> their inclusion on iron is a poor match when used with the underlying 6-31G or 6-311G basis sets. Water was chosen as the solvent because the electron and proton reference energies were defined in an aqueous environment. We did perform additional calculations with a dielectric constant to better model an active site environment. However, while the absolute energies changed, the key results obtained remained consistent. Using these calculated free energies as well as the chemical potentials of a solvated free electron (with respect to a SHE reference state) and proton (in a dilute aqueous environment), the half-reaction free energies were obtained as per the approach outlined by Llano and Eriksson.<sup>44</sup>

## RESULTS AND DISCUSSION

In order to evaluate the mechanistic feasibility of the various possible iron–oxygen oxidants, we began by first examining the inherent free-energy cost of oxidizing the R group Im of histidine (modeled as Im) via either an ET or a PCET process. In the SHE reference state, the loss of an electron from Im to give the radical cation  $\text{Im}^{\bullet+}$  is endothermic by 186.0 kJ mol<sup>-1</sup> (Table 1). However, the coupling of ET with proton loss from

**Table 1. Adiabatic Free Energies (kJ mol<sup>-1</sup>) for Oxidation of the Im via ET and PCET**

ET	species formed	PCET	species formed
186.0(189.5)	$\text{Im}^{\bullet+}$	171.0 (163.3)	$\text{ImN}_\delta(-\text{H})^\bullet$
		250.1 (238.6)	$\text{ImC}_\delta(-\text{H})^\bullet$
		251.5 (241.2)	$\text{ImC}_\epsilon(-\text{H})^\bullet$

either the  $\text{C}_\delta\text{-H}$  or  $\text{C}_\epsilon\text{-H}$  moieties of the Im, i.e., PCET to give a deprotonated neutral Im-derived radical [ $\text{Im}(-\text{H})^\bullet$ ], is markedly even more endothermic with free-energy costs of 250.1 and 251.5 kJ mol<sup>-1</sup>, respectively.

As previously noted,<sup>17</sup> in the resulting radical species [i.e.,  $\text{ImC}_\delta(-\text{H})^\bullet$  and  $\text{ImC}_\epsilon(-\text{H})^\bullet$ ], the unpaired electron is localized on the respective carbon as an  $\text{sp}^2$  radical.<sup>17</sup> However, while the alternate PCET process involving proton loss from the Im's  $\text{N}_\delta\text{-H}$  group is still endothermic, the free-energy cost is significantly lower at 171.0 kJ mol<sup>-1</sup>. In fact, it is now less than that of the ET process alone (see Table 1)! Again, as noted previously,<sup>17</sup> in the resulting  $\text{ImN}_\delta(-\text{H})^\bullet$  radical, the unpaired electron is delocalized over the  $\pi$  system of the Im itself.<sup>17</sup> As noted above, the formation of 2- and 5-HisCysSO is believed to follow similar chemistries. Thus, it seems that, of the above three possible processes, the formation of  $\text{ImN}_\delta(-\text{H})^\bullet$  is thermodynamically most favored.

While  $\text{Fe}^{\text{IV}}=\text{O}$  is generally considered the stronger oxidant, we first investigated the free energies of reducing the various possible ferrous dioxygen complexes (**A**), shown in Figure 1, via an ET or a PCET process. For each complex, we calculated the energies and geometries of the singlet (biradical), triplet, quintet, and septet multiplicities. Notably, each **A** complex was found to prefer a septet GS with the iron center in its ferric state ( $\text{Fe}^{\text{III}}$ ), with the bound dioxygen moiety better represented as a superoxide radical,  $\text{O}_2^{\bullet-}$ . Furthermore, in each complex (except for **A**<sub>4</sub>), the dioxygen was bound side-on. These results agree with previous computational investigations.<sup>4,61</sup> In particular, Chen et al.<sup>4</sup> found that for [(TMC)- $\text{O}_2\text{Fe}^{\text{II}}$ ]<sup>2+</sup> the septet GS was preferred with dioxygen bound side-on. In addition, Chung et al.<sup>61</sup> found that in several nonheme complexes the septet GS was preferred. However, the

side- or end-on binding of dioxygen depended on the steric crowding about the iron.<sup>61</sup> For reduction of the **A** complexes via ET, we calculated the energies and geometries of the doublet, quartet, and sextet complexes. The reduction of each **A** complex via a single ET is endothermic by at least 60.4 kJ mol<sup>-1</sup> (Table 2). In the case of **A**<sub>5</sub>, reduction via ET caused cleavage

**Table 2. Adiabatic Free Energies (kJ mol<sup>-1</sup>) for Reduction of the  $\text{Fe}^{\text{III}}\text{O}_2^{\bullet-}$  Complexes (**A**) via ET or PCET**

complex	ET <sup>62</sup>	PCET <sup>62</sup>
<b>A</b> <sub>1</sub>	89.1	-57.7 (-55.2)
<b>A</b> <sub>2</sub>	76.6	-55.6 (-42.6)
<b>A</b> <sub>3</sub>	73.0	-59.3 (-62.0)
<b>A</b> <sub>4</sub>	60.4	-84.7 (-87.4)
<b>A</b> <sub>5</sub>	NA	-63.1 (-64.1)
<b>A</b> <sub>6</sub>	80.2	-76.5 (-78.3)
<b>A</b> <sub>7</sub>	66.4	-77.6 (-86.5)

of an  $\text{Fe}\cdots\text{Im}$  ligation and, thus, the resulting complex was ignored in further studies. With reduction, it was found that the preferred state was no longer solely the high-spin state. While for **A**<sub>1</sub>, **A**<sub>6</sub>, and **A**<sub>7</sub>, the sextet state was preferred, for **A**<sub>2</sub>, **A**<sub>3</sub>, and **A**<sub>4</sub>, the quartet state was favored. The resulting spin and charge densities imply that the added electron goes onto the iron center, thus resulting in a ferrous superoxo ( $\text{Fe}^{\text{II}}\text{O}_2^{\bullet-}$ ) complex.

In contrast, if ET is coupled with PT (i.e., a PCET) to the distal oxygen of the bound dioxygen, reduction of the **A** complexes becomes exothermic (Table 2). Like reduction via ET, we investigated formation of the doublet, quartet, and sextet multiplicities. It is noted that the free energies for reduction via PCET, whereby the proton was localized on the proximal oxygen, were also calculated. However, the energies obtained were 50 kJ mol<sup>-1</sup> less exothermic than those provided in Table 2 and thus will not be discussed hereafter. In all cases, it was found that upon reduction via PCET the resulting complexes **A**<sub>1</sub>–**A**<sub>7</sub> preferred the quartet multiplicity. The resulting spin and charge densities suggest the formation of ferric peroxide ( $\text{Fe}^{\text{III}}\text{OOH}$ ) complexes. Chung et al.<sup>61</sup> have suggested that the oxidizing power of  $\text{Fe}^{\text{III}}\text{O}_2^{\bullet-}$  is related to the energy of the  $\pi^*(\text{O}_2)$  orbital (i.e., the orbital that the added electron populates). More specifically, the lower its energy, the greater the free-energy change for reduction.<sup>61</sup> Thus, it is perhaps not surprising that ET is endothermic while PCET is significantly exothermic given the different moieties into which the added electron goes. Of the **A** complexes considered, the most powerful oxidant (**A**<sub>4</sub>; Figure 1) is the only one in which the dioxygen moiety is bound to the iron end-on. Furthermore, a  $\text{H}_2\text{O}$  molecule is ligated to the iron trans to the carboxylate, while the cysteine is monodentately bound via its sulfur. However, the free energy of reduction of **A**<sub>4</sub> via a PCET process is only -84.7 kJ mol<sup>-1</sup> (Table 2). This is not in itself sufficient to overcome the free energy required to oxidize the Im (171.0 kJ mol<sup>-1</sup>). Thus, it appears unlikely that any of the  $\text{Fe}^{\text{III}}\text{O}_2^{\bullet-}$  complexes are suitable mechanistic oxidants.

Next, we considered the free energy associated with reduction of the possible  $\text{Fe}^{\text{IV}}=\text{O}$ -containing complexes (**B**) shown in Figure 2. Using the optimized structures of the **A** complexes, we manually cleaved the O–O bond with concomitant S=O bond formation. Again, we considered all possible relevant multiplicities. For each complex, we calculated the energies and geometries of the singlet, triplet, and quintet multiplicities. Unlike **A** (which were found to all exist in the



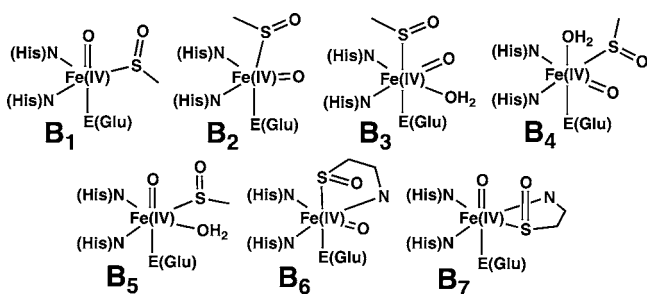


**Figure 2.** Initial five- and six-coordinate  $\text{Fe}^{\text{IV}}=\text{O}$  complexes considered herein.

septet), it was found that  $\text{B}_2$ ,  $\text{B}_4$ ,  $\text{B}_5$ , and  $\text{B}_7$  were found to have a triplet GS, while a quintet GS was favored in  $\text{B}_1$ ,  $\text{B}_3$ , and  $\text{B}_6$ . Interestingly, in the latter three complexes, the cysteine sulfur is ligated to the iron trans to the carboxylate. Previous investigations of  $\text{Fe}^{\text{IV}}=\text{O}$  complexes have noted that a triplet GS is generally favored.<sup>16,61,63–82</sup> All complexes preferred a quintet GS at the M06/6-311G(2df,p)//B3LYP/6-31G(d) level.

Upon reduction via ET, all of the resulting anionic complexes had a sextet GS (in comparison to quartet and doublet systems) except those arising from  $\text{B}_1$  and  $\text{B}_5$ , which instead had a quartet GS. For the high-spin anions, the calculated spin and charge densities indicated formation of an  $\text{Fe}^{\text{III}}\text{O}^-$  complex. For the majority of the reduced complexes, the iron coordination environment was disrupted. Specifically, in  $\text{B}_3$ ,  $\text{B}_4$ , and  $\text{B}_5$ ,  $\text{H}_2\text{O}$  was no longer ligated to the iron center but instead hydrogen-bonded to the  $\text{Fe}^{\text{III}}\text{O}^-$  moiety and either the sulfoxide or carboxylate oxygen. For  $\text{B}_2$  and  $\text{B}_7$ , an  $\text{Fe}\cdots\text{Im}$  ligation was broken, with the Im instead hydrogen bonding to  $\text{Fe}^{\text{III}}\text{O}^-$  and either the sulfoxide's amine or  $\text{S}=\text{O}$  oxygen. Only for those anions arising from  $\text{B}_1$  and  $\text{B}_6$  did the iron center retain its coordination. As observed for the above  $\text{Fe}^{\text{III}}\text{O}_2^{\bullet-}$  complexes, reduction of all  $\text{Fe}^{\text{IV}}=\text{O}$  species via ET is endothermic (Table 3). Now, however, the process is, on

**Table 3.** Adiabatic Free Energies ( $\text{kJ mol}^{-1}$ ) for Reduction of the  $\text{Fe}^{\text{IV}}=\text{O}$  Complexes (**B**) via ET or PCET

complex	ET <sup>62</sup>	PCET <sup>62</sup>
$\text{B}_1$	90.0	−126.6 (−130.2)
$\text{B}_2$	65.7	−114.1 (−128.8)
$\text{B}_3$	38.7	−143.0 (−143.4)
$\text{B}_4$	57.9	−143.9 (−136.1)
$\text{B}_5$	44.4	−146.5 (−126.5)
$\text{B}_6$	69.1	−139.6 (−156.3)
$\text{B}_7$	67.5	−116.2 (−139.6)

average, less endothermic. For example, for  $\text{B}_3$ , reduction via ET costs just  $38.7 \text{ kJ mol}^{-1}$ . This differs from that observed by Chung et al.,<sup>61</sup> where the  $\text{Fe}^{\text{III}}\text{O}_2^{\bullet-}$  complexes had higher electron affinities.

In contrast, reduction of the  $\text{Fe}^{\text{IV}}=\text{O}$  complexes (**B**) via PCET did not disrupt the iron's six-coordinate ligation. However, there was again variation in the preferred GS multiplicity of the resulting complexes. While, in general, the quartet state was favored,  $\text{B}_2$ ,  $\text{B}_3$ , and  $\text{B}_6$  instead had a sextet GS. For the high-spin complexes, the calculated spin densities indicated formation of an  $\text{Fe}^{\text{III}}\text{OH}$  complex. Energetically, reduction via PCET was again found to be exothermic. Now, however, it is considerably more favored by at least  $31 \text{ kJ mol}^{-1}$

than that seen for the **A** ( $\text{Fe}^{\text{III}}\text{O}_2^{\bullet-}$ ) complexes. Yet still, their exothermicity, or oxidant power, is insufficient to overcome the inherent cost ( $171.0 \text{ kJ mol}^{-1}$ ) associated with oxidizing Im.

Previously, de Visser and Straganz<sup>83</sup> have investigated computationally the enzyme cysteine dioxygenase (CDO), which catalytically dioxygenates a cysteine. While CDO has three ligating Im, a key intermediate in the mechanism is a  $\text{Fe}^{\text{IV}}=\text{O}\cdots\text{sulfoxide}$  complex (as proposed in OvoA and EgtB). Importantly, they observed that a mechanistic intermediate containing an  $\text{Fe}-\text{OO}-\text{S}$  linkage that forms prior to  $\text{O}-\text{O}$  homolytic bond cleavage. Thus, we considered the redox abilities of seven such intermediate complexes (**C**) for our present models (Figure 3). Using the optimized structures of

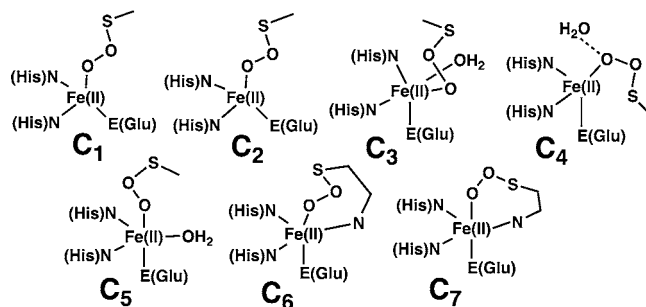


**Figure 3.** Initial five- and six-coordinate ferrylperoxysulfur complexes considered herein.

the **A** complexes, we formed an  $\text{S}-\text{O}$  bond. For each new **C** complex, we calculated the geometries and energies (see the Computational Methods section) for the singlet, triplet, and quintet multiplicities. It is noted that  $\text{C}_6$  and  $\text{C}_7$  are analogous to those obtained by de Visser and Straganz (i.e., bidentate ligation of cysteine).<sup>83</sup> All **C** complexes were found to prefer a quintet GS, with the calculated spin densities suggesting that the iron is in a 2+ oxidation state. In agreement with previous studies,<sup>83</sup> in the optimized structures of each of the **C**-type complexes, no  $\text{Fe}\cdots\text{S}$  interaction was observed. It is noted that as a result the iron center's coordination geometries in  $\text{C}_1$  and  $\text{C}_2$  are quite similar with a distorted trigonal-bipyramidal geometry. In particular, the peroxy moiety was essentially trans to the carboxylate ligand. In the case of  $\text{C}_4$ , the  $\text{H}_2\text{O}$  also dissociated from the iron center and instead hydrogen-bonded to the proximal oxygen of the ferrous peroxy-sulfur moiety.

Unlike the previous systems, free energies of reduction via ET could not be obtained because the addition of an electron to each **C** complex resulted in their collapse to mechanistically infeasible complexes. As for the  $\text{Fe}^{\text{III}}\text{O}_2^{\bullet-}$  and  $\text{Fe}^{\text{IV}}=\text{O}$  complexes, reduction of the  $\text{FeOOS}$  complexes via a PCET was thermodynamically favorable (Table 4). However, the

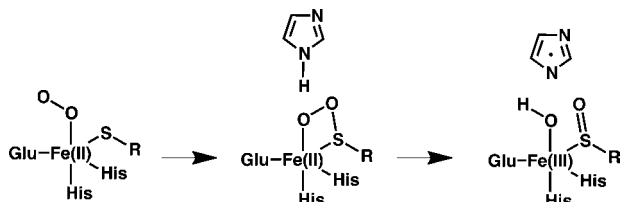
**Table 4.** Adiabatic Free Energies ( $\text{kJ mol}^{-1}$ ) for Reduction of the  $\text{FeOOS}$  Complexes (**C**; See Figure 6) via PCET

complex	PCET <sup>62</sup>
$\text{C}_1$	−211.1 (−274.1)
$\text{C}_2$	−205.3 (−195.1)
$\text{C}_3$	−203.9 (−214.6)
$\text{C}_4$	−215.2 (−245.4)
$\text{C}_5$	−265.1 (−284.9)
$\text{C}_6$	−208.7 (−238.8)
$\text{C}_7$	−268.3 (−308.4)

exothermicity of the process is now significantly greater. Indeed, all FeOOS complexes have potentials around or above 200 kJ mol<sup>-1</sup>. Thus, they are all now capable of oxidizing Im to give an ImN<sub>δ</sub>(-H)<sup>•</sup> radical. In such cases, subsequent C-S bond formation would require a formal proton shuttle from C<sub>δ</sub>-H or C<sub>ε</sub>-H to give the 2- or 5-HisCysSO product. Interestingly, however, both computational methods indicate that several of the complexes are, in fact, sufficiently strong enough to oxidize histidine via a PCET to directly form HisC<sub>δ</sub>(-H)<sup>•</sup> or HisC<sub>ε</sub>(-H)<sup>•</sup>. This would allow for C-S bond formation without the need for an intramolecular proton shuttle.

Upon reduction of each of the FeOOS complexes in Figure 3, the peroxy O-O bond was cleaved, resulting in the formation of complexes containing an iron-oxygen species with an iron-bound sulfoxide! Specifically, for C<sub>2</sub>, C<sub>3</sub>, C<sub>4</sub>, and C<sub>5</sub>, the complex formed contained an Fe<sup>II</sup>OH moiety and a weakly interacting sulfoxide radical, while for C<sub>1</sub>, C<sub>6</sub>, and C<sub>7</sub>, it contained an Fe<sup>III</sup>OH moiety with a bound sulfoxide. It is noted that the need for sulfoxidation by OvoA and EgtB in the C-S bond formation has previously puzzled experimentalists.<sup>17</sup> This is partly due to the fact that formation of a sulfoxide moiety appears unnecessary for subsequent steps and, furthermore, it is not present in the final product.<sup>17,18,20,84</sup> The results obtained herein using small model iron complexes suggest that formation of a sulfoxide could be a consequence of the reduction of a powerful mechanistic FeOOS oxidant in order to oxidize the histidine cosubstrate. As noted in the Introduction, the use of such model biomimetic iron complexes does not conclusively elucidate the mechanisms of enzymes such as OvoA or EgtB. However, they can provide fundamental insight into the oxidative power of the iron center in such systems and its dependence upon its coordination. Given the current model systems, a possible pathway for enzymes such as OvoA and EgtB that involves the most thermodynamically favored intermediates is given in Scheme 2. Once further experimental data in particular structures are obtained for relevant enzyme complexes, their mechanisms can be elucidated in detail.

**Scheme 2. Proposed Intermediates for the Formation of Histidyl Sulfoxide Based on Thermodynamic Stability**



## CONCLUSION

In summary, oxidation of histidine was thermodynamically most favorable for the formation of a HisN<sub>δ</sub>(-H)<sup>•</sup> radical via a PCET process. Of the small model iron-oxygen oxidants considered, only the ferrous peroxysulfur (i.e., FeOOS) complexes were found to be inherently capable of performing this oxidation. Furthermore, several such complexes were also able to oxidize histidine to generate the higher-energy radicals HisC<sub>δ</sub>(-H)<sup>•</sup> and HisC<sub>ε</sub>(-H)<sup>•</sup>. Importantly, from the results, the need to form sulfoxide is rather a consequence of the formation of a more powerful oxidant in the model FeOOS

complexes, providing insight into the puzzling need for sulfoxidation.

## ASSOCIATED CONTENT

### Supporting Information

The xyz coordinates of the optimized structures of all A-C complexes investigated herein (Table S1). This material is available free of charge via the Internet at <http://pubs.acs.org>.

## AUTHOR INFORMATION

### Corresponding Author

\*E-mail: [gauld@uwindsor.ca](mailto:gauld@uwindsor.ca).

### Notes

The authors declare no competing financial interest.

## ACKNOWLEDGMENTS

We thank the Canada Foundation for Innovation and the Ontario Innovation Trust for funding and SHARCNET for additional computational resources. E.A.C.B. also thanks NSERC for a PGS-D scholarship.

## REFERENCES

- (1) Kovaleva, E. G.; Lipscomb, J. D. *Nat. Chem. Biol.* **2008**, *4*, 186–193.
- (2) Yi, C. Q.; Jia, G. F.; Hou, G. H.; Dai, Q.; Zhang, W.; Zheng, G. Q.; Jian, X.; Yang, C. G.; Cui, Q. A.; He, C. A. *Nature* **2010**, *468*, 330–U223.
- (3) Klinman, J. P. *Acc. Chem. Res.* **2007**, *40*, 325–333.
- (4) Chen, H.; Cho, K.-B.; Lai, W.; Nam, W.; Shaik, S. J. *Chem. Theory Comput.* **2012**, *8*, 915–926.
- (5) Bollinger, J. M.; Krebs, C. *Curr. Opin. Chem. Biol.* **2007**, *11*, 151–158.
- (6) Buijninx, P. C. A.; van Koten, G.; Gebbink, R. *Chem. Soc. Rev.* **2008**, *37*, 2716–2744.
- (7) Galonić Fujimori, D.; Barr, E. W.; Matthews, M. L.; Koch, G. M.; Yonce, J. R.; Walsh, C. T.; Bollinger, J. M.; Krebs, C.; Riggs-Gelasco, P. J. *J. Am. Chem. Soc.* **2007**, *129*, 13408–13409.
- (8) Karlsson, A.; Parales, J. V.; Parales, R. E.; Cibson, D. T.; Eklund, H.; Ramaswamy, S. *Science* **2003**, *299*, 1039.
- (9) Krebs, C.; Galonić Fujimori, D.; Walsh, C. T.; Bollinger, J. M. *Acc. Chem. Res.* **2007**, *40*, 484–492.
- (10) Matthews, M. L.; Krest, C. M.; Barr, E. W.; Vaillancourt, F. d. r. H.; Walsh, C. T.; Green, M. T.; Krebs, C.; Bollinger, J. M. *Biochemistry* **2009**, *48*, 4331–4343.
- (11) Mbughuni, M. M.; Chakrabarti, M.; Hayden, J. A.; Bominaar, E. L.; Hendrich, M. P.; Munck, E.; Lipscomb, J. D. *Proc. Natl. Acad. Sci. U.S.A.* **2010**, *107*, 16788–16793.
- (12) Nam, W. *Acc. Chem. Res.* **2007**, *40*, 465–465.
- (13) Cho, K. B.; Chen, H.; Janardanan, D.; de Visser, S. P.; Shaik, S.; Nam, W. *Chem. Commun.* **2012**, *48*, 2189–2191.
- (14) van der Donk, W. A.; Krebs, C.; Bollinger, J. M. *Curr. Opin. Struct. Biol.* **2010**, *20*, 673–683.
- (15) Gupta, R.; Lacy, D. C.; Bominaar, E. L.; Borovik, A. S.; Hendrich, M. P. *J. Am. Chem. Soc.* **2012**.
- (16) de Visser, S. P. *Angew. Chem., Int. Ed.* **2006**, *45*, 1790–1793.
- (17) Braunschhausen, A.; Seebeck, F. P. *J. Am. Chem. Soc.* **2011**, *133*, 1757–1759.
- (18) Seebeck, F. P. *J. Am. Chem. Soc.* **2010**, *132*, 6632–6633.
- (19) Que, L. *Nat. Struct. Biol.* **2000**, *7*, 182–184.
- (20) Vogt, R. N.; Spies, H. S. C.; Steenkamp, D. J. *Eur. J. Biochem.* **2001**, *268*, 5229–5241.
- (21) Turner, E.; Klevit, R.; Hager, L. J.; Shapiro, B. M. *Biochemistry* **1987**, *26*, 4028–4036.
- (22) Shapiro, B. M.; Hopkins, P. B. *Adv. Enzymol. Relat. Areas Mol. Biol.* **1991**, *64*, 291–316.

- (23) Rohl, I.; Schneider, B.; Schmidt, B.; Zeeck, E. *Z. Naturforsch. C* **1999**, *54*, 1145–1147.
- (24) Ariyanayagam, M. R.; Fairlamb, A. H. *Mol. Biochem. Parasitol.* **2001**, *115*, 189–198.
- (25) Cheah, I. K.; Halliwell, B. *Biochim. Biophys. Acta, Mol. Basis Dis.* **2012**, *1822*, 784–793.
- (26) Aruoma, O. I.; Spencer, J. P. E.; Mahmood, N. *Food Chem. Toxicol.* **1999**, *37*, 1043–1053.
- (27) Ey, J.; Schomig, E.; Taubert, D. *J. Agric. Food Chem.* **2007**, *55*, 6466–6474.
- (28) Cheah, I. K.; Halliwell, B. *Biochim. Biophys. Acta, Mol. Basis Dis.* **2012**, *1822*, 784–793.
- (29) Hartman, P. E. *Method Enzymol.* **1990**, *186*, 310–318.
- (30) Akanmu, D.; Cecchini, R.; Aruoma, O. I.; Halliwell, B. *Arch. Biochem. Biophys.* **1991**, *288*, 10–16.
- (31) Zhu, B.-Z.; Mao, L.; Fan, R.-M.; Zhu, J.-G.; Zhang, Y.-N.; Wang, J.; Kalyanaraman, B.; Frei, B. *Chem. Res. Toxicol.* **2010**, *24*, 30–34.
- (32) Hand, C. E.; Taylor, N. J.; Honek, J. F. *Bioorg. Med. Chem. Lett.* **2005**, *15*, 1357–1360.
- (33) Rahman, I.; Gilmour, P. S.; Jimenez, L. A.; Biswas, S. K.; Antonicelli, F.; Aruoma, O. I. *Biochem. Biophys. Res. Commun.* **2003**, *302*, 860–864.
- (34) Kirkham, P.; Rahman, I. *Pharmacol. Ther.* **2006**, *111*, 476–494.
- (35) Asmus, K. D.; Bensasson, R. V.; Bernier, J. L.; Houssin, R.; Land, E. J. *Biochem. J.* **1996**, *315*, 625–629.
- (36) Shapiro, B. M. *Science* **1991**, *252*, 533–536.
- (37) Holler, T. P.; Hopkins, P. B. *J. Am. Chem. Soc.* **1988**, *110*, 4837–4838.
- (38) Zoete, V.; Bailly, F.; Catteau, J. P.; Bernier, J. L. *J. Chem. Soc., Perkin Trans. 1* **1997**, 2983–2988.
- (39) Zoete, V.; Bailly, F.; Vezin, H.; Teissier, E.; Duriez, P.; Fruchart, J. C.; Catteau, J. P.; Bernier, J. L. *Free Radical Res.* **2000**, *32*, 515–+.
- (40) Zoete, V.; Vezin, H.; Bailly, F.; Vergoten, G.; Catteau, J. P.; Bernier, J. L. *Free Radical Res.* **2000**, *32*, 525–+.
- (41) Jacob, C. *Nat. Prod. Rep.* **2006**, *23*, 851–863.
- (42) Krauth-Siegel, R. L.; Bauer, H.; Schirmer, H. *Angew. Chem., Int. Ed.* **2005**, *44*, 690–715.
- (43) Spies, H. S. C.; Steenkamp, D. J. *Eur. J. Biochem.* **1994**, *224*, 203–213.
- (44) Llano, J.; Eriksson, L. A. *J. Chem. Phys.* **2002**, *117*, 10193–10206.
- (45) Frisch, M. J.; Trucks, G. W.; Schlegel, H. B.; Scuseria, G. E.; Robb, M. A.; Cheeseman, J. R.; Scalmani, G.; Barone, V.; Mennucci, B.; Petersson, G. A.; Nakatsuji, H.; Caricato, M.; Li, X.; Hratchian, H. P.; Izmaylov, A. F.; Bloino, J.; Zheng, G.; Sonnenberg, J. L.; Hada, M.; Ehara, M.; Toyota, K.; Fukuda, R.; Hasegawa, J.; Ishida, M.; Nakajima, T.; Honda, Y.; Kitao, O.; Nakai, H.; Vreven, T.; Montgomery, J. A., Jr.; Peralta, J. E.; Ogliaro, F.; Bearpark, M.; Heyd, J. J.; Brothers, E.; Kudin, K. N.; Staroverov, V. N.; Keith, T.; Kobayashi, R.; Normand, J.; Raghavachar, K.; Rendell, A.; Burant, J. C.; Iyengar, S. S.; Tomasi, J.; Cossi, M.; Rega, N.; Millam, J. M.; Klene, M.; Knox, J. E.; Cross, J. B.; Bakken, V.; Adamo, C.; Jaramillo, J.; Gomperts, R.; Stratmann, R. E.; Yazyev, O.; Austin, A. J.; Cammi, R.; Pomelli, C.; Ochterski, J. W.; Martin, R. L.; Morokuma, K.; Zakrzewski, V. G.; Voth, G. A.; Salvador, P.; Dannenberg, J. J.; Dapprich, S.; Daniels, A. D.; Farkas, O.; Foresman, J. B.; Ortiz, J. V.; Cioslowski, J.; Fox, D. J. *Gaussian 09*; Gaussian, Inc.: Wallingford, CT, 2010.
- (46) Hirao, H. *J. Phys. Chem. B* **2011**, *115*, 11278–11285.
- (47) Hirao, H.; Morokuma, K. *J. Phys. Chem. Lett.* **2010**, *1*, 901–906.
- (48) Becke, A. D. *J. Chem. Phys.* **1993**, *98*, 1372.
- (49) Becke, A. D. *J. Chem. Phys.* **1993**, *98*, 5648–5652.
- (50) Handy, N. C.; Cohen, A. J. *Mol. Phys.* **2001**, *99*, 403–412.
- (51) Lee, C. T.; Yang, W. T.; Parr, R. G. *Phys. Rev. B* **1988**, *37*, 785–789.
- (52) Stephens, P. J.; Devlin, F. J.; Chabalowski, C. F.; Frisch, M. J. *J. Phys. Chem.* **1994**, *98*, 11623–11627.
- (53) Vosko, S. H.; Wilk, L.; Nusair, M. *Can. J. Phys.* **1980**, *58*, 1200–1211.
- (54) Cancès, E.; Mennucci, B.; Tomasi, J. *J. Chem. Phys.* **1997**, *107*, 3032–3041.
- (55) Mennucci, B.; Cancès, E.; Tomasi, J. *J. Phys. Chem. B* **1997**, *101*, 10506–10517.
- (56) Mennucci, B.; Tomasi, J. *J. Chem. Phys.* **1997**, *106*, 5151–5158.
- (57) Tomasi, J.; Mennucci, B.; Cancès, E. *THEOCHEM* **1999**, *464*, 211–226.
- (58) Zhao, Y.; Truhlar, D. G. *Theor. Chem. Acc.* **2008**, *120*, 215–241.
- (59) Zhao, Y.; Truhlar, D. G. *Acc. Chem. Res.* **2008**, *41*, 157–167.
- (60) Martin, J.; Baker, J.; Pulay, P. *J. Comput. Chem.* **2009**, *30*, 881–883.
- (61) Chung, L. W.; Li, X.; Hirao, H.; Morokuma, K. *J. Am. Chem. Soc.* **2011**, *133*, 20076–20079.
- (62) Free energies for ET were calculated via the equation  $\text{Ox}(\text{aq}) + e^-(\text{aq})(\text{SHE}) = \text{Red}(\text{aq})$ . Free energies for PCET were calculated via the equation  $\text{Ox}(\text{aq}) + \text{H}^+(\text{aq}) + e^-(\text{aq})(\text{SHE}) = \text{Red}(\text{aq})$ .
- (63) Bassan, A.; Borowski, T.; Siegbahn, P. E. M. *Dalton Trans.* **2004**, 3153–3162.
- (64) Blomberg, L. M.; Blomberg, M. R. A.; Siegbahn, P. E. M. *J. Biol. Inorg. Chem.* **2004**, *9*, 923–935.
- (65) Borowski, T.; Blomberg, M. R. A.; Siegbahn, P. E. M. *Chem.—Eur. J.* **2008**, *14*, 2264–2276.
- (66) de Visser, S. P. *J. Am. Chem. Soc.* **2006**, *128*, 9813–9824.
- (67) de Visser, S. P. *J. Am. Chem. Soc.* **2010**, *132*, 1087–1097.
- (68) Decker, A.; Rohde, J. U.; Klinker, E. J.; Wong, S. D.; Que, L.; Solomon, E. I. *J. Am. Chem. Soc.* **2007**, *129*, 15983–15996.
- (69) Geng, C. Y.; Ye, S. F.; Neese, F. *Angew. Chem., Int. Ed.* **2010**, *49*, 5717–5720.
- (70) Hirao, H.; Kumar, D.; Que, L.; Shaik, S. *J. Am. Chem. Soc.* **2006**, *128*, 8590–8606.
- (71) Hirao, H.; Morokuma, K. *J. Am. Chem. Soc.* **2009**, *131*, 17206–17214.
- (72) Hirao, H.; Morokuma, K. *J. Am. Chem. Soc.* **2010**, *132*, 17901–17909.
- (73) Hirao, H.; Que, L.; Nam, W.; Shaik, S. *Chem.—Eur. J.* **2008**, *14*, 1740–1756.
- (74) Johansson, A. J.; Blomberg, M. R. A.; Siegbahn, P. E. M. *J. Chem. Phys.* **2008**, *129*.
- (75) Lai, W. Z.; Shaik, S. *J. Am. Chem. Soc.* **2011**, *133*, 5444–5452.
- (76) Latifi, R.; Bagherzadeh, M.; de Visser, S. P. *Chem.—Eur. J.* **2009**, *15*, 6651–6662.
- (77) Lundberg, M.; Kawatsu, T.; Vreven, T.; Frisch, M. J.; Morokuma, K. *J. Chem. Theory Comput.* **2009**, *5*, 222–234.
- (78) Michel, C.; Baerends, E. J. *Inorg. Chem.* **2009**, *48*, 3628–3638.
- (79) Neidig, M. L.; Decker, A.; Choroba, O. W.; Huang, F.; Kavana, M.; Moran, G. R.; Spencer, J. B.; Solomon, E. I. *Proc. Natl. Acad. Sci. U.S.A.* **2006**, *103*, 12966–12973.
- (80) Salomon, O.; Reiher, M.; Hess, B. A. *J. Chem. Phys.* **2002**, *117*, 4729–4737.
- (81) Shaik, S.; Chen, H.; Janardanan, D. *Nat. Chem.* **2011**, *3*, 19–27.
- (82) Ye, S.; Neese, F. *Proc. Natl. Acad. Sci. U.S.A.* **2011**, *108*, 1228–1233.
- (83) de Visser, S. P.; Straganz, G. D. *J. Phys. Chem. A* **2009**, *113*, 1835–1846.
- (84) Ishikawa, Y.; Israel, S. E.; Melville, D. B. *J. Biol. Chem.* **1974**, *249*, 4420–4427.